Polarizations for proton knockout reactions from $s_{1/2}$ orbits at 1 GeV

V. A. Andreev,[1] M. N. Andronenko,[1] G. M. Amalsky,[1] S. L. Belostotski,[1] O. A. Domchenkov,[1] O. Ya. Fedorov,[1] K. Hatanaka,[2] A. A. Izotov,[1] A. A. Jgoun,[1] J. Kamiya,[2] A. Yu. Kisselev,[1] M. A. Kopytin,[1] O. V. Miklukho,[1] Yu. G. Naryshkin,[1] T. Noro,[3,*] E. Obayashi,[2] A. N. Prokofiev,[1] D. A. Prokofiev,[1] H. Sakaguchi,[4] V. V. Sulimov,[1] A. V. Shvedchikov,[1] H. Takeda,[4] S. I. Trush,[1] V. V. Vikhrov,[1] T. Wakasa,[2] Y. Yasuda,[4] H. P. Yoshida,[2] and A. Zhdanov[1]

[1]*Petersburg Nuclear Physics Institute, Gatchina 188350, Russia*

[2]*Research Center for Nuclear Physics, Osaka University, Ibaraki 567-0047, Japan*

[3]*Department of Physics, Kyushu University, Fukuoka 812-8581, Japan*

[4]*Department of Physics, Kyoto University, Kyoto 606-8502, Japan*

(Received 14 February 2003; revised manuscript received 14 August 2003; published 19 February 2004)

The polarization of protons emitted in $(p,2p)$ reactions has been measured for three kinds of targets at 1 GeV. The values of the polarization that we obtain are significantly smaller than the values predicted using the nucleon-nucleon (*NN*) interaction in free space, and the discrepancy between the two is seen to increase monotonically as a function of the effective mean density, which is defined as a measure of the sensitivity of a reaction to density-dependent terms of the interaction. The experimental data are also compared with a model calculation that includes a relativistic effect, and it is found that inclusion of this effect is able to account for about half of the density-dependent discrepancy between the experimental results and the values predicted with the free space *NN* interaction. These results, in conjunction with the previous results at 392 MeV, indicate that this discrepancy is not caused by a contribution of multistep processes and provide further evidence that there exists a medium effect.

DOI: 10.1103/PhysRevC.69.024604 PACS number(s): 25.40.−h, 21.30.Fe, 24.50.+g, 24.70+s

I. INTRODUCTION

The modification of basic properties of nucleons and mesons in nuclear fields is one of the most interesting current topics in nuclear and hadron physics. It has been predicted in the framework of quantum chromodynamics that nucleon and meson masses are modified as a result of the partial restoration of chiral symmetry in nuclear media [1–3]. From a different viewpoint, it has been conjectured that a nucleon Dirac spinor is modified in nuclear matter due to the large scalar potential in the framework of quantum hadrodynamics [4]. This modification, a lower-component enhancement of the Dirac spinor, is also expressed as a decrease of nucleon masses in a nuclear field. Because nucleon-nucleon (*NN*) interactions are described as meson exchange forces between nucleons, it is expected that such medium effects at the hadron level cause modification of *NN* interactions that is detectable with some nuclear reactions.

Intensive efforts have been continued to study *NN* interactions in the nuclear field and to investigate the effects of possible modification of hadron properties. In the study of nucleon elastic scattering, significant success has been realized with the relativistic impulse approximation [5–7], in which a modification of the Dirac spinor is implicitly taken into account. The effect of meson-mass modification on proton-nucleus scattering has been investigated by Brown *et al.* [8], and they found that the theoretical prediction is improved when this effect is taken into account. Recently, Sakaguchi *et al.* [9] studied this effect experimentally and concluded that modifications of the coupling constants and meson masses in the *NN* interaction are necessary in order to obtain predictions consistent with their experimental data in the case that the relativistic impulse approximation is employed. For inelastic scattering, various kinds of medium effects have been examined using experimental data that include spin observables by Sammarruca and co-workers [10]. There are also works in which the relativistic effect on the effective interaction is examined for both elastic and inelastic scattering consistently [11,12].

Another type of nuclear reaction suitable for studying in-medium *NN* interactions is nucleon quasifree scattering which is, in a simple picture, *NN* scattering in a nuclear field. It was first pointed out clearly in a theoretical paper [4], based on LAMPF data [13] from inclusive measurements, that the analyzing power A_y values measured are smaller than those predicted using the free *NN* interaction. It has been suggested that this decrease in A_y is a signature of the relativistic effect mentioned above. This decrease has also been found to be much more distinct, for a $(p,2p)$ reaction corresponding to proton knockout from the $1s_{1/2}$ orbit of a ^{16}O target in a TRIUMF experiment with an incident energy of 500 MeV [14]. Maxwell and Cooper analyzed these data with a relativistic distorted wave impulse approximation (DWIA) formalism that includes both dynamic and kinematical recoil effects [15]. Although their formalism exactly includes the relativistic effect that was crudely treated in Ref. [4], yet the calculated A_y values for knockout from the $1s_{1/2}$ state and the experimental data are in significant disagreement. They also found that the elimination of the spin-orbit parts of the Schrödinger phase-equivalent distortion potential gives moderate outgoing-proton energy dependence of the calculated A_y for $1s_{1/2}$ knockout, which is closer to the experimental data. On the other hand, Krein *et al.* have inves-

*Electronic address: noro@nucl.phys.kyushu-u.ac.jp

tigated the effects of modifications of meson masses and coupling constants on *NN* interactions in nuclear field. They have found that the effective polarizations of the target nucleons derived from data for $^{16}O(p,2p)$ reactions at an incident energy of 200 MeV leading to $p_{3/2}$ and $p_{1/2}$ hole states [16] can be consistently accounted for if such modified *NN* interactions are employed [17].

Experiments on $(p,2p)$ reactions have been made for several types of target nuclei at 392 MeV by an experimental group at RCNP [18]. As in the case of the above TRIUMF data, the A_y data for $1s_{1/2}$ knockout are found to be smaller than those estimated by using *NN* interactions in free space. In addition, they found that the decreasing rates are significantly target dependent. They defined an effective mean density that provides a good measure of the sensitivity of a $(p,2p)$ reaction to the density-dependent term of *NN* interactions and showed that the observed decrease of A_y monotonically depends on the mean density. This result strongly suggests the existence of a medium effect on *NN* interactions in nuclear fields. It has also been shown that this density-dependent reduction cannot be accounted for by a medium effect in the nonrelativistic framework, which is inclusion of the Pauli-blocking effect [19]. In a recent paper, Miller *et al.* compare the TRIUMF data with results of "the best available DWIA reaction models" [20]. They conclude that the existing density-dependent *NN* interactions are not adequate for nucleon knockout reactions and the possibility of a more interesting mechanism, such as a hadron level medium effect, is implied.

In this paper, we present the results of new measurements of the polarization parameter *P* for $(p,2p)$ reactions at 1 GeV, which is a significantly higher energy than those of the previous measurements made at TRIUMF and RCNP. At this energy, the polarization for the knockout of *s*-shell and *p*-shell protons in the $^7Li(p,2p)$ reaction were recently measured, and found to be suppressed, especially significant for *s*-shell knockout, compared with values obtained with a simple impulse approximation [21]. One purpose of the present study is to investigate the target dependence, which essentially represents a density dependence, of this suppression for *s*-shell knockout. In addition, we have measured the angular distribution of polarizations for a ^{12}C target for an angular range where outgoing energies change significantly: from 750 MeV to 890 MeV for forward outgoing protons and from 130 MeV to 210 MeV for backward outgoing protons. The second purpose of this experiment is to study this phenomenon over a wide range of energies, in which the contributions of multistep processes are believed to vary significantly. This angular distribution gives the polarizations for a significantly wide range of the recoil momentum values compared with the scale of typical meson-mass values in the meson exchange model of the *NN* interaction. It is also intended to provide a test for examination of theoretical models that predict modifications of the in-medium *NN* interaction, which may be related to medium effects at the hadron level.

II. EXPERIMENTAL DETAILS AND RESULT

A. Beam and spectrometers

The experiment was carried out using a 1-GeV proton beam produced by the synchrocyclotron at the Petersburg Nuclear Physics Institute (PNPI), Gatchina. The accelerated proton beam was focused on the center of the scattering chamber of a two-arm spectrometer system. The diameter of the beam was about 10 mm. The CH_2, ^6Li, C, and Ca targets, with a typical size of 8 mm wide $\times 12$ mm high $\times 4$ mm thick, were held by a system of fibers.

TABLE I. Properties of the magnetic spectrometers.

	MAP	NES
Maximum momentum (GeV/*c*/*Z*)	1.7	1.0
Central orbit radius (m)	5.5	3.27
Deflection angle (deg)	24.0	37.2
Momentum dispersion (m)	2.2	2.4
Solid angle (msr)	0.40	3.1
Momentum acceptance (%)	8.0	8.0

Two outgoing protons in $(p,2p)$ reactions, as well as the *p*-*p* scattering in the case of the CH_2 target, were momentum analyzed in coincidence using the spectrometer system that consists of a pair of QQD-type magnetic spectrometers, called MAP and NES. The ion-optical properties of these spectrometers are listed in Table I, and a schematic depiction of the experimental setup is given in Fig. 1. In the focal plane of each spectrometer, two sets of multiwire proportional chambers (MWPC's), labeled PC1 and PC2 in the figure, were used to measure positions and with this information, the momenta of detected protons were deduced.

Throughout the $(p,2p)$ measurement, the angles and field strengths of the spectrometers were set at those corresponding to the zero-recoil condition for *s*-shell knockout from each target nucleus. This is the condition for which the cross section for *s*-shell knockout is maximal and the reaction mechanism is expected to be the simplest.

Figure 2 displays typical spectra for the four kinds of targets. Because thick targets were used in this experiment,

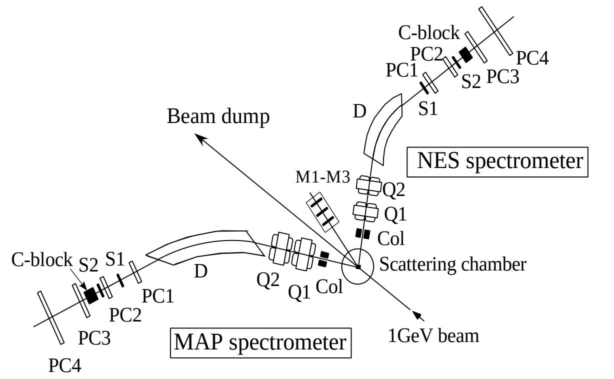

FIG. 1. Schematic diagram of the two-arm spectrometer system at PNPI. Four sets of MWPCs (PC1–PC4), two trigger scintillators (S1 and S2), and a carbon analyzer block form a focal-plane polarimeter system on each spectrometer. Each of PC1–PC4 consists of two MWPCs for measurements of horizontal and vertical positions. Collimators (Col) are positioned in front of the spectrometers, and the luminosity is monitored using a beam monitor that consists of three scintillators (M1–M3).

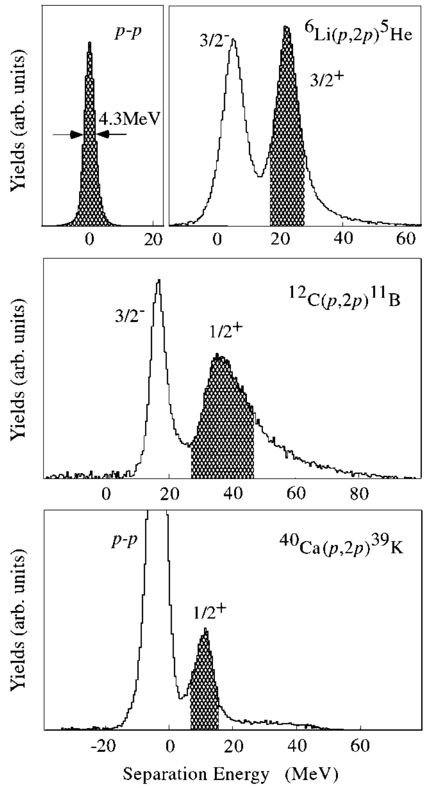

FIG. 2. Separation energy spectra for *p*-*p* scattering and $(p,2p)$ reactions. The shaded areas were used for data analysis. The accidental coincidence events have been subtracted and a correction has been made for the energy-loss effect. See the text for the explanation of the unphysical position of the *p*-*p* peak in the bottom panel.

both the incident and outgoing protons suffered significant energy losses. All the spectra shown are those after the energy-loss effect, typically 3–4 MeV in total, is corrected. In the case of the ^{40}Ca target, *p*-*p* scattering from the supporting fiber was observed simultaneously. Because the energy loss occurring in these events is significantly smaller than that in $(p,2p)$ events taking place in the target block, and because the correction for the energy loss was made assuming that all the events occur in the target block, the position of the *p*-*p* peak is shifted to the left relative to the actual energy in the figure. The overall energy resolution for the *p*-*p* measurement was 4.3 MeV, as shown in the figure. The number of accidental coincidence events was estimated using coincidence events between adjacent beam bunches, and this number has been subtracted in the figure. Typical ratios of true to accidental events for the shaded area are 15:1 and 1:1 for ^{6}Li and ^{12}C target nuclei, respectively. The data from the shaded area were used for further analysis.

B. Polarization measurement

Besides the two sets of MWPCs mentioned above, a carbon block was placed for polarization analysis of detected protons. The *p*-C scattering off the carbon block was traced using two additional sets of MWPCs, PC3 and PC4, and the polarization of detected protons was deduced from the left-right asymmetry of the scattering. The polarization P for the $(p,2p)$ reactions was calculated as

$$P = \frac{\sum_{i=1}^{n_{t+a}} \cos\,\phi_i - \frac{1}{N}\sum_{i=1}^{n_a} \cos\,\phi_i}{\sum_{i=1}^{n_{t+a}} A_y(\theta_i)\cos^2\phi_i - \frac{1}{N}\sum_{i=1}^{n_a} A_y(\theta_i)\cos^2\phi_i},$$

where n_{t+a} is the number of events that correspond to the "true" beam-bunch peak in the distribution of the time differences between the MAP and NES signals, which include both true and accidental events. The number of events that correspond to N accidental beam bunches is denoted as n_a. The scattering angle and azimuthal angle for the *p*-C scattering of the ith event are represented by θ_i and ϕ_i, respectively, and $A_y(\theta_i)$ is the effective analyzing power of the analyzer.

The actual ranges of θ used depend on the energy of the protons and also on the interaction point in the analyzer, because the acceptance angle depends on the position. The maximum ranges for the MAP and NES spectrometers were 3.5°–18° and 5.5°–22°, respectively. The thickness of the carbon block was varied between 3 cm and 20 cm related to the energy of detected protons. For $A_y(\theta)$, the compiled results of a PNPI group [22] and a TRIUMF group [23] were used.

C. Experimental results

The results of the polarization measurement are tabulated in Table II. In the table, values of the effective mean density $\overline{\rho}/\rho_0$, which is defined in Ref. [18], and the momentum transfer q are given, as well as detection angles and energies. The actual calculation of the effective mean density was carried out following a procedure described in Ref. [18] using the computer code THREEDEE [24], with minor modifications.

In Fig. 3, some of the data for four kinds of targets are plotted as functions of $\overline{\rho}/\rho_0$. The data plotted here correspond to a detection angle of the NES spectrometer of around 53.3°. As described above, the angle of the MAP spectrometer and the fields of both spectrometers were adjusted so that the two protons that pass the central orbits of the two spectrometers correspond to those resulting from $(p,2p)$ reactions that lead to the peak of the $s_{1/2}$-hole states, $1s_{1/2}$ for ^{6}Li and ^{12}C targets, and $2s_{1/2}$ for ^{40}Ca, with the zero-recoil condition.

Figure 4 displays the angular distributions for the ^{12}C$(p,2p)$ reaction and *p*-*p* scattering. The data corresponding to NES angles of 63.9°, 59.7°, and 53.3° are plotted as functions of the transferred momentum q. The MAP angles and both fields were set to yield conditions similar to those described above.

For *p*-*p* scattering, the polarization of forward outgoing protons P_1 should be the same as that of backward outgoing protons P_2 excluding a minor contribution resulting from parity-violating interactions. As seen in the figure, at each value of q considered, the measured values or P_1 and P_2 for *p*-*p* scattering are equal within the statistical errors of 0.01–0.02. Moreover, these data are consistent with the result of a phase shift analysis [25] for *p*-*p* scattering, that is represented by the dot-dashed curve in Fig. 4. The agreement

TABLE II. Detection angles Θ_1 and Θ_2, kinetic energies T_1 and T_2, and measured polarizations P_1 and P_2, of forward and backward outgoing protons measured in the present experiment. The values of the momentum transferred q by forward scattered particles and estimated mean density $\overline{\rho}$ in units of the saturation density (ρ_0=0.18 fm^{-3}) are also given. The recoil momenta for these $(p,2p)$ conditions are effectively zero. The $(p,2p)$ data for ^{6}Li and ^{12}C targets at an NES angle Θ_2=53.3° represent the mean values of the measurements at 53.1° and 53.5°, while the corresponding *p*-*p* data are listed separately. The ^{12}C data at 63.9° also represent the averages of values measured at 63.7° and 64.0°.

Target	Θ_1(deg)	Θ_2(deg)	T_1(MeV)	T_2(MeV)	q (fm^{-1})	P_1	P_2	$\overline{\rho}/\rho_0$
^{1}H	17.6	64.0	866	134	2.63	0.445±0.011	0.453±0.023	
	20.9	59.7	817	183	3.11	0.428±0.010	0.437±0.010	
	25.8	53.5	737	263	3.80	0.326±0.012	0.327±0.008	
	26.1	53.1	730	270	3.86	0.338±0.006	0.320±0.007	
^{6}Li	24.0	53.3	741	238	3.58	0.305±0.019	0.260±0.019	0.19
^{12}C	13.2	63.9	878	87	2.02	0.274±0.059		0.34
	17.1	59.7	833	132	2.60	0.296±0.032	0.198±0.068	0.32
	22.7	53.3	747	218	3.42	0.270±0.032	0.194±0.032	0.31
^{40}Ca	25.1	53.1	734	255	3.74	0.305±0.034	0.269±0.031	0.07

found between these results indicate that the effective analyzing power used is sufficient, and systematic errors are not dominant.

In the situation depicted in Fig. 3, the values of the polarization for the $(p,2p)$ reactions are smaller than those for *p*-*p* scattering by an amount that increases and becomes significant with increasing effective mean density. The ^{12}C data, which correspond to the largest densities, are plotted as a function of q in Fig. 4.

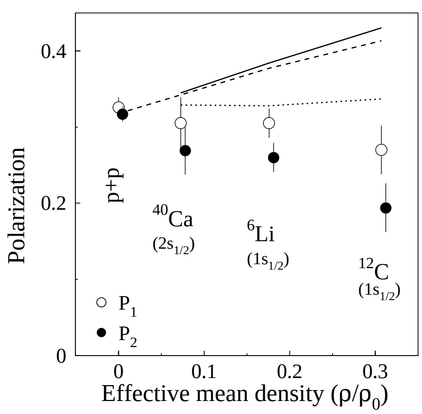

FIG. 3. Target dependence of the polarization data for *p*-*p* scattering and $(p,2p)$ reactions. The polarizations of forward and backward outgoing protons are denoted by P_1 and P_2, respectively. The data are plotted as functions of the effective mean density defined in Ref. [18]. The data points for P_2 are shifted slightly to the right to avoid overlapping. The dashed curve and the solid curve represent results of the PWIA and DWIA calculations with the *NN* interaction in free space, respectively. The dashed curve is extended to $\overline{\rho}/\rho_0$ =0 where the value of the polarization is obtained from phase shift analysis [25] for *p*-*p* scattering. The dotted curve is the DWIA result, in which the relativistic effect is taken into account in a Schrödinger-equivalent form.

III. COMPARISON WITH THEORETICAL PREDICTIONS AND DISCUSSIONS

In this section, first the data are compared with the results of nonrelativistic PWIA, plane wave impulse approximation, and DWIA calculations employing an on-shell factorized approximation. The dashed curves and solid curves, corresponding to PWIA and DWIA, respectively, in both Figs. 3 and 4 represent the results of the calculations, which were obtained using the computer code THREEDEE [24]. A global optical potential [26], parametrized in the relativistic framework and converted to the Schrödinger-equivalent form, was used to calculate the distorted waves of incident and outgoing protons in the case of DWIA, and a conventional well-depth method was used to construct bound-state wave functions. Because the difference between P_1 and P_2 values in

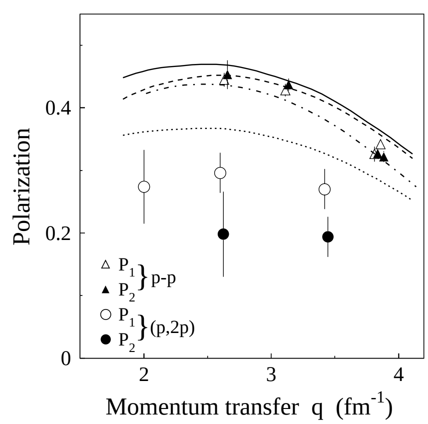

FIG. 4. Angular dependence of the polarization for *p*-*p* scattering and the ^{12}C$(p,2p)$ reaction. P_1 and P_2 are the polarizations of forward and backward outgoing protons, respectively. The data are plotted as functions of the momentum transfer. The dot-dashed curve represents the result of a phase shift analysis [25] for the *p*-*p* scattering. The identifications of the other curves are the same as those in Fig. 3.

the DWIA calculations was found to be small, typically smaller than 0.01 and no more than 0.02, only the P_1 values obtained from DWIA are plotted in these figures. As seen in the figures, the difference between the PWIA and DWIA results is quite small. This result suggests that the distortion, in a conventional nonrelativistic framework, does not play an essential role in the polarization for the kinematic conditions employed in the present work. It is noted here that the difference between the dot-dashed curve and the dashed curve in Fig. 4 is caused by the difference between the two-body kinematics of *p*-*p* scattering and $(p,2p)$ reactions with finite Q values. The final energy prescription was used for the impulse approximation (IA) calculations. We also found that the difference between the initial and final prescriptions was small in these kinematic regions. The strong positive slope of the polarizations predicted by these calculations in Fig. 3 is caused by the kinematic effects of the binding energy of the struck proton.

The difference between the values from the IA calculations and the measured polarizations, both of P_1 and P_2, are monotonically increasing functions of the effective mean density. This result is similar to the corresponding result obtained at 392 MeV [18] with regard to the analyzing power and it provide further evidence that there exists a medium effect. In this figure, it is seen that the experimental values of P_1 and P_2 are, respectively, $\approx$63% and 45% as large as the IA values for $^{12}C(p,2p)$. These differences for the $^{12}C(p,2p)$ reaction are essentially constant over the entire range of angles for the data plotted in Fig. 4, where the mean density is also almost constant. Note here that there is a systematic difference between the P_1 and P_2 values, though they have the same value in the case of elastic *p*-*p* scattering, as mentioned above. Possible origins of the finite difference between these values include nonrelativistic and relativistic distortions (though the former is excluded if the present DWIA calculations are valid), contributions of multistep processes, and even nontrivial modification of nucleons in the nuclear field. However, the differences are within twice of the magnitude of the statistical errors and are considerably smaller than the differences between either dataset and the results of the DWIA calculations. In this paper, therefore, we treat P_1 and P_2 equal and consider only the main features of their discrepancies from the theoretical predicted values.

Next, the data are compared with a theoretical result in the case that a relativistic effect, the distortion of the nucleon spinor, is taken into account. The calculation was carried out in the Schrödinger-equivalent form. More specifically, this calculation consists of a nonrelativistic DWIA calculation with a nucleon-nucleon t matrix, that is modified in the nuclear potential following a procedure similar to that proposed by Horowitz and Iqbal [4].

In the relativistic framework, the T matrix for a $(p,2p)$ reaction is given by

$$T = F_k \int \overline{\Psi}_1(\mathbf{r})\overline{\Psi}_2(\mathbf{r})\hat{F}\Phi(\mathbf{r})\Psi_0(\mathbf{r})d\mathbf{r},$$

where $\Psi_i(\mathbf{r})$ is the four-component wave function of an incident $(i=0)$ or outgoing $(i=1,2)$ proton. Here, $\Phi(\mathbf{r})$ is the wave function of the bound nucleon. The Lorenz invariant *NN* amplitude is represented by $\hat{F}$, and F_k is a kinematic factor.

Now, we express this T matrix in Schrödinger-equivalent form as

$$T = F_k \int \chi_1^\dagger(\mathbf{r})\chi_2^\dagger(\mathbf{r})\langle\overline{U_1}\,\overline{U_2}|\hat{F}|U_3U_0\rangle\phi(\mathbf{r})\chi_0(\mathbf{r})d\mathbf{r}.$$

Here, the quantities $\chi_i(\mathbf{r})$ and $\phi(\mathbf{r})$ are two-component wave functions, and U_i are defined by $\Psi_i(\mathbf{r})=U_i\chi_i(\mathbf{r})$ and $\Phi(\mathbf{r})=U_3\phi(\mathbf{r})$. This expression is obtained when we replace the momentum operator in the lower component of U_i with the corresponding asymptotic momentum values. Then the quantity $\langle\overline{U_1}\,\overline{U_2}|\hat{F}|U_3U_0\rangle$ is simply equated with the t matrix in the Schrödinger framework in free space. In a nuclear field, the effect of the nucleon effective mass is taken into account through U_i, while $\hat{F}$ is assumed to be unchanged, independent of the nuclear density.

In the present calculations, a linear dependence of the effective mass of nucleons on the nuclear density is assumed, and the value of the mass corresponding to the effective mean density, represented by the abscissa in Fig. 3, is used for each target. The value of the effective mass at the saturation density is taken to be 0.56 of the nucleon mass in free space [27]. The results of the calculations are plotted in Figs. 3 and 4 by the dotted curves. It is found that the discrepancy between the predictions obtained from those calculations and the experimental values is roughly half as large as that between the predictions obtained with the free *NN* interaction and the experimental values. The result is also similar to that found at 392 MeV for the analyzing power [28] and thus it implies that the same kinds of mechanism causes the density-dependent modification of these observables at both energies. It is also to be emphasized that this calculation gives an almost constant reduction rate in Fig. 4, where the effective mean density is practically the same.

It is noted here that this treatment of the relativistic effect does not necessarily yield predictions consistent with experimental results for other kinds of spin observables for this reaction. At 392 MeV, several kinds of spin transfer coefficients have been measured and compared with the results of similar calculations [29]. In some cases, the calculation gives predictions that deviate from the experimental values by even more than predictions obtained from simple DWIA calculations with the *NN* interaction in free space. At present, however, this kind of medium effect is the only mechanism known to account for the discrepancies: strong density dependence, weak momentum-transfer dependence, and also weak incident-energy dependence. It is important to note that the nonrelativistic medium effect fails to account for these features [19].

Another possible medium effect is the modification of $\hat{F}$. Krein *et al.* have shown that modifications of exchanged meson masses and coupling constants in the relativistic Love-Franey (RLF) model [30] cause significant changes in spin observables which include suppressions of A_y. Because parameter values for the RLF model valid in the 1-GeV region are not known, such a calculation is not presented in this paper, but this effect is expected to lead to smaller predicted values of P.

In this kind of medium effect, the discrimination of meson-mass effects and coupling constant effects may be important. In the RLF model, the amplitudes $\hat{F}$ are written as sums of Yukawa functions with cutoff parameters in momentum space,

$$\frac{g_j^2}{q^2 + m_j^2}(1 + q^2/\Lambda_j^2)^2,$$

where m_j is the mass of an exchanged j meson, q is the transferred momentum, g_j^2 is the coupling constant of this meson exchange force, and Λ_j is the cutoff parameter. It may be possible to make the discrimination between these effects by comparing the results of calculations with data over a wide range of values of q. Because the range of values of q in Fig. 4 is significantly wide compared with typical mass values of exchanged mesons, the comparison of experimental data with the results of calculations allows us to discriminate modification of g_j and m_j from the q dependence, although it may be difficult to extract such information from the present data because of their fairly large uncertainties. Further experimental studies at this energy should provide a good test to identify the origin of the density dependence.

IV. SUMMARY AND CONCLUSIONS

We have measured polarizations of forward and backward outgoing protons in $(p,2p)$ reactions at an incident energy of 1 GeV. The measurements were made for proton knockout from the $s_{1/2}$ orbits of ^{6}Li, ^{12}C, and ^{40}Ca target nuclei, $1s_{1/2}$ for ^{6}Li and ^{12}C targets, and $2s_{1/2}$ for ^{40}Ca. The kinematics for the measurement were selected to satisfy the zero-recoil condition, in which case the effects of ambiguities in the nuclear structure and the reaction mechanism are expected to be small.

The values we measured for the polarization are significantly smaller than those obtained from the PWIA and DWIA calculations employing free space *NN* interactions. We also found that the discrepancy between these theoretical values and our experimental values increases monotonically with the effective mean density, which is a quantity that provides a means by which to measure the sensitivity of the cross section to the density-dependent term of *NN* interactions. The data were also compared with the results of a calculation in which the relativistic effect is taken into account with a Schrödinger-equivalent form, and it was found that the effective mass accounts for almost half of the density-dependent discrepancy between the experimental and theoretical results. These results are similar to the results of previous works investigating the analyzing power for the same reactions at an incident energy of 392 MeV.

For the polarization of ^{12}C$(p,2p)$, the angular distribution was also measured. The data show almost constant reductions from the IA calculations, independent of momentum transfer and outgoing energies. In this case as well, the relativistic effect accounts for half of this discrepancy.

From the fact that essentially the same reduction rate has been observed over wide ranges of incident and outgoing protons, in which contributions of multistep processes are expected to vary significantly, it is concluded that this phenomenon does not originate from the reaction mechanism. In order to extract a definitive conclusion regarding the medium modification of interactions, more theoretical works are needed. The data presented here should provide a good test for such works.

ACKNOWLEDGMENTS

We thank the members of the accelerator group at PNPI for their support. The Japanese authors of this work are indebted to the PNPI staff members for their warm hospitality during the time that the experiment was being conducted. This program is supported by grants-in-aid from the Ministry of Education, Science, Sports and Culture and from the Yamada Science Foundation. It is also partially supported by the Russian Foundation for Basic Research Grant No. 02-02-17142.

[1] G. E. Brown and M. Rho, Phys. Rev. Lett. **66**, 2720 (1991).
[2] R. J. Furnstahl, D. K. Griegel, and T. D. Cohen, Phys. Rev. C **46**, 1507 (1992).
[3] T. Hatsuda, Nucl. Phys. **A544**, 27c (1992).
[4] C. J. Horowitz and M. J. Iqbal, Phys. Rev. C **33**, 2059 (1986).
[5] D. P. Murdock and C. J. Horowitz, Phys. Rev. C **35**, 1442 (1987).
[6] J. A. Tjon and S. J. Wallace, Phys. Rev. C **36**, 1085 (1987).
[7] N. Ottenstein, S. J. Wallace, and J. A. Tjon, Phys. Rev. C **38**, 2272 (1988).
[8] G. E. Brown, A. Sethi, and N. M. Hintz, Phys. Rev. C **44**, 2653 (1991).
[9] H. Sakaguchi *et al.*, Phys. Rev. C **57**, 1749 (1998).
[10] F. Sammarruca, E. J. Stephenson, K. Jiang, J. Liu, C. Olmer, A. K. Opper, and S. W. Wissink, Phys. Rev. C **61**, 014309 (1999), and references therein.
[11] R. J. Furnstahl and S. J. Wallace, Phys. Rev. C **47**, 2812 (1993).
[12] J. J. Kelly and S. J. Wallace, Phys. Rev. C **49**, 1315 (1994).
[13] J. A. McGill *et al.*, Phys. Lett. **134B**, 157 (1984).
[14] C. A. Miller *et al.*, in *Proceedings of the 7th International Conference on Polarization Phenomena in Nuclear Physics*, Paris, 1990 (Editions de Physique, Les Vlis, France, 1990), p. C6–595.
[15] O. V. Maxwell and E. D. Cooper, Nucl. Phys. **A574**, 819 (1994).
[16] P. Kitching, C. A. Miller, W. C. Olsen, D. A. Hutcheon, W. J. McDonald, and A. W. Stetz, Nucl. Phys. **A340**, 423 (1980).
[17] G. Krein, Th. A. J. Maris, B. B. Rodrigues, and E. A. Veit, Phys. Rev. C **51**, 2646 (1995).

[18] K. Hatanaka *et al.*, Phys. Rev. Lett. **78**, 1014 (1997).
[19] T. Noro *et al.*, Nucl. Phys. **A663&A664**, 517c (2000).
[20] C. A. Miller *et al.*, Phys. Rev. C **57**, 1756 (1998).
[21] O. V. Miklukho *et al.*, Nucl. Phys. **A683**, 145 (2001).
[22] O. Fedorov, LNPI Report No. 484, 1973, p. 1.
[23] G. Waters *et al.*, Nucl. Instrum. Methods **153**, 401 (1978).
[24] N. S. Chant and P. G. Roos, Phys. Rev. C **27**, 1060 (1983).
[25] R. A. Arndt, I. I. Strakovsky, and R. L. Workman, Phys. Rev. C **62**, 034005 (2000).
[26] E. D. Cooper, S. Hama, B. C. Clark, and R. L. Mercer, Phys. Rev. C **47**, 297 (1993).
[27] D. Serot and J. D. Walecka, *in Advances in Nuclear Physics*, edited by J. W. Negele and E. Vogt (Plenum, New York, 1986), Vol. 16.
[28] T. Noro *et al.*, Nucl. Phys. **A629**, 324c (1998).
[29] T. Noro, in *Spin 2000*, edited by Hiroyaru Ejiri, Kichiji Hatanoka, Kenichi Imai, and Takashi Nakano, AIP Conf. Proc. No. 570 (AIP, Melville, NY, 2001), p. 228.
[30] C. J. Horowitz, Phys. Rev. C **31**, 1340 (1985).